LAWRENCE
LIVERMORE
NATIONAL
LABORATORY

LLNL-JRNL-849536

VanOp_GR_paper_v004

R. J. Deri, E. Deri, W. E. Fenwick, S. H. Baxamusa, J. Li, N. P. Allen, D. Mittelberger, R. B. Swertfeger, S. J. Telford, M. C. Boisselle, D. L. Pope, D. M. Dutra, L. Martin, L. Gilmore, G. Thaler, M. Crowley, P. Thiagarajan

May 25, 2023

Semiconductor Science and Technology

Disclaimer

This document was prepared as an account of work sponsored by an agency of the United States government. Neither the United States government nor Lawrence Livermore National Security, LLC, nor any of their employees makes any warranty, expressed or implied, or assumes any legal liability or responsibility for the accuracy, completeness, or usefulness of any information, apparatus, product, or process disclosed, or represents that its use would not infringe privately owned rights. Reference herein to any specific commercial product, process, or service by trade name, trademark, manufacturer, or otherwise does not necessarily constitute or imply its endorsement, recommendation, or favoring by the United States government or Lawrence Livermore National Security, LLC. The views and opinions of authors expressed herein do not necessarily state or reflect those of the United States government or Lawrence Livermore National Security, LLC, and shall not be used for advertising or product endorsement purposes.

Determination of Nonradiative Carrier Lifetimes in Quantum Well Laser Diodes from Subthreshold Characteristics

R.J. Deri[1)*], E. McVay[1)*], W.E. Fenwick[1a)*], S.H. Baxamusa[1)*], J. Li[1)], N.P. Allen[1)], D. Mittelberger[1)], R.B. Swertfeger[1)], S.J. Telford[1)], M.C. Boisselle[1)], D.L. Pope[1)], D.M. Dutra[1)], L. Martin[1)], L. Gilmore[1)], G. Thaler[2)], M. Crowley[2)], J. Song,[2)] and P. Thiagarajan[2)]

[1]*Lawrence Livermore National Laboratory, 7000 East Avenue, Livermore CA 94550*
[2]*Leonardo Electronics US Inc, 7775 N. Casa Grande Highway, Tucson AZ 85743*
[*]These authors contributed equally to the manuscript

Abstract
A method for determination of non-radiative carrier lifetimes in the waveguide and active regions of quantum well laser diodes is presented. This method is suitable for characterization of fully packaged devices and requires no special measurement equipment if the device structure is known. The proposed approach is experimentally demonstrated for several 800 nm laser diodes.

1. Introduction

Methods to measure nonradiative lifetimes of free carriers in edge-emitting, semiconductor laser diodes are of interest to assess degradation of their power and efficiency due to nonradiative recombination. There is particular interest in measurement techniques for fully packaged devices, so that changes in nonradiative behavior due to aging and other stresses can be monitored non-destructively. Because access to packaged devices is only possible through the emitting diode facet, lifetime measurement techniques such as time-resolved photoluminescence cannot be applied. Van Opdorp[1] previously demonstrated a method to determine the nonradiative lifetime of the active layer in double-heterostructure laser diodes from only the subthreshold power-current characteristic under forward bias, without the need for absolute calibration of the optical collection efficiency of the measurement system. The simplicity of this approach, which requires only standard measurement equipment, renders it highly attractive; however, its applicability to modern laser diodes using quantum well gain media is not straightforward. Here we describe how this approach can be extended to separate confinement, quantum well lasers to determine nonradiative carrier lifetimes in both the quantum well and waveguide regions.

[a] Author to whom correspondence should be addressed: fenwick2@llnl.gov

2. Background

The original Van Opdorp method employs the measured spontaneous emission to quantify the carrier density in the gain medium. For optical collection efficiency C of the metrology system, it can be shown that the carrier density in the gain medium is

$$N = \left(\frac{L}{CBV^*}\right)^{\frac{1}{2}} \tag{1}$$

where L is the detected optical output (photons/sec), V* is the gain medium volume, and B is the radiative recombination coefficient (cm^{-3}/s) in the gain medium. Assuming that all of the applied current I is injected into the gain medium, it can be shown that the L-I relationship follows

$$\frac{I}{eL} = \frac{1}{C} + \left(\frac{1}{\tau}\sqrt{\frac{CV^*}{B}}\right)L^{-\frac{1}{2}} \tag{2}$$

for radiative efficiency eL/I, nonradiative lifetime τ, and electron charge e.[1] A fit of data to the linear relationship between I/eL and $1/L^{1/2}$ yields both the collection efficiency and the nonradiative lifetime, provided B has been established by other means (such as time-resolved photoluminescence experiments or simulations). The linearity of (2) breaks down at high injection due to amplification of spontaneous emission and Auger recombination, and breaks down at very low bias as injected carrier densities approach intrinsic carrier density levels. The range of linear behavior shall be referred to as the Van Opdorp linear range.

Extension of this approach to quantum well (QW) laser diodes is complicated by the imperfect injection efficiency $\eta_{inj} = I_{QW}/I$, which causes the current consumed in the QW I_{QW} to differ appreciably from the applied current I. Following the same approach as van Opdorp[1], it can be shown that

$$\frac{I}{eL} = \frac{1}{C^*} + \left(\frac{1}{\eta_{inj}^{\frac{1}{2}}\,\tau_{QW}}\sqrt{\frac{C^*V^*}{B}}\right)L^{-\frac{1}{2}} \tag{3}$$

where $C^* = \frac{C}{\eta_{inj}}$. Experimentally, such linear behavior is observed over a broad range of bias conditions for QW laser diodes, as shown in Figure 1. If the injection efficiency were independent of bias current, this approach would provide a scaled measure of nonradiative lifetime $\eta_{INJ}^{1/2}\tau_{QW}$. Unfortunately, the injection efficiency is expected to vary significantly with bias. As a result, using this linear fit approach can significantly underestimate τ_{QW}, even if the injection efficiency is known.

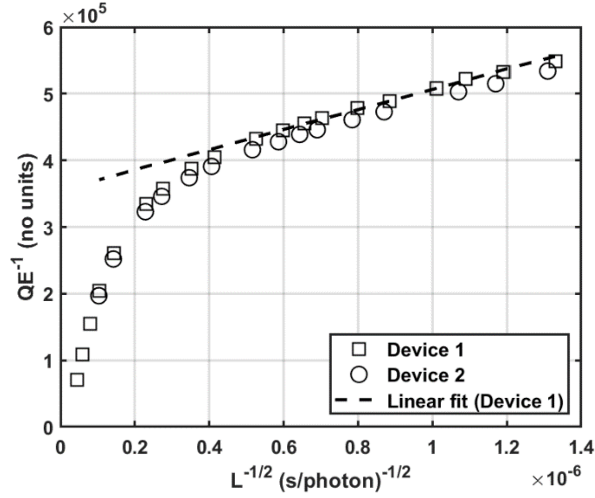

Figure 1: Typical plot of quantum efficiency QE versus light output L, plotted in linearized form following Eq. (3) for two quantum well laser diode bars emitting near 800 nm. The dashed line shows the linear fit to the Device 1 data set over bias currents ranging from 50-250 mA.

3. Methodology

Adaptation of this approach to QW laser diodes requires determination of the current I_{SCH} that is not injected into the quantum well, so that the injection efficiency can be determined from

$$I = I_{SCH} + I_{QW} \qquad (4)$$

The current I_{SCH} includes contributions from recombination in the waveguide region surrounding the QW gain medium, as well as other contributions such as drift currents (recombination in highly doped regions), radiative recombination, and leakage currents. In general, it can be described by

$$I_{SCH}(V) = I_0(V) + \frac{1}{\tau_{WG}} I_{WG}(V) \qquad (5)$$

where the $I_{WG}(V)$ term (with coefficient I_{WG} having units of A-s) accounts for nonradiative recombination in the waveguide region with a lifetime τ_{WG}, and the $I_0(V)$ term accounts for all other currents. Both of these contributions depend on the bias voltage V. The expression for waveguide recombination is approximate, and is strictly valid only when either electron and hole densities or recombination lifetimes are equal.[2] Drift-diffusion simulations can be used to determine the parameters $I_0(V)$ and $I_{WG}(V)$,[3] based on the device structure and material parameters.[b]

---

[b] At low densities, the quantum well density scales almost as $\ln\left(1 + \exp\left(\frac{F}{kT}\right) \sim \exp\left(\frac{F}{kT}\right)\right.$, for imref F sufficiently below the band edge (F<0). Since the density nearly follows Boltzmann statistics for the low carrier densities present when the linear relationship Eq. (3) holds, conventional simulators incorporating only 3-dimensional material models can be used for this purpose.

Once $I_0(V)$ and $I_{WG}(V)$ have been established, nonradiative lifetimes τ_{QW} and τ_{WG} in the QW and waveguide regions can be extracted from measured power-voltage-current behavior in the Van Opdorp linear regime. For a data set where the Kth datapoint consists of a measured current, voltage, and light output (I_K, V_K, L_K), we expect that the observed current will be given by

$$I_K = I_0(V_K) + \frac{1}{\tau_{WG}} I_{WG}(V_K) + eV^* \left(\frac{N(L_K)}{\tau_{QW}} + BN(L_K)^2 + C_{Aug} N(L_K)^3 \right) \qquad (6)$$

with QW density $N(L_K) = \left(\frac{L_K}{C\ B\ V^*}\right)^{\frac{1}{2}}$ and QW Auger coefficient C_{Aug}. Provided at least three datapoints K are available, one can solve Eq. (6) to determine the three parameters τ_{QW}, τ_{WG} and C. When more than three datapoints are available, these parameters are determined by an optimization that minimizes the sum of the residual errors between the measured I_K and model fit (right hand side of Eq. (6)).

4. Experimental

This method was used to characterize the nonradiative lifetimes in separate confinement heterostructure, single-QW laser diode bars. The bars are fabricated from phosphide-based epitaxial materials grown on GaAs by solid-source molecular beam epitaxy. The epitaxial layer structure comprises a single quantum well embedded in a 1.1 μm thick waveguide layer which is sandwiched between highly doped n- and p-type cladding materials. CV measurements indicate a net residual donor density in the waveguide of $1\text{x}10^{15}$ cm^{-3}. The bars are 1 cm wide, have 1.5 mm cavity length, and contain twelve 200 μm wide emitting diode stripes. The bars are soldered p-side down to CuW submounts that are mounted to a temperature-controlled stage held at 20 °C. Additional details of these devices are reported elsewhere.[4] The bars lase near 800 nm wavelength with typical threshold current of 7.8 A. Subthreshold data was collected using standard laser diode metrology, with special care to remove series resistance effects from the voltage data using 4-wire metrology and corrections for the measured resistance of dummy package structures. Optical power values were converted to photon fluxes L_K using the centroids of the measured emission spectra.

The subthreshold photon flux output dependence on drive current was measured for four devices. All devices showed the characteristic linear dependence of I/eL vs. $L^{-1/2}$ expected from (3) over a current range from 50 to 250 mA, as shown in Figure 1. Deviations at high currents result from amplification of the spontaneous emission at higher carrier densities. The bias voltage over this current range varied from

1.47 to 1.56 V. In this range, the I-V characteristic can be described by an ideality factor n~1.38. This value is significantly lower than the n>1.8 value observed at lower bias (≤1.2V) for these devices[4] due to appreciable contributions from QW radiative recombination to the overall current.

5. Results and discussion

5.1 Fitting procedure

The subthreshold L-I-V data was analyzed by fitting to (6) using coefficients $I_0(V)$ and $I_{WG}(V)$ determined from a 1-dimensional drift-diffusion (DD) simulator. The simulations employed a device structure using a waveguide bandgap of 1.900 eV deduced from photoluminescence data,[5] quantum well composition determined from X-ray diffraction and properties determined from k·p simulations (Heterostructure Design Studio, www.optronics.com).[6] Additional structural details have been previously reported.[4] The QW radiative recombination coefficient B=2.8 x10^{-10} cm^3/s was determined from k·p simulations of optical absorption vs. carrier density, using standard methods.[7] The doping profile in the structure was determined from capacitance-voltage profiling. Other material parameters were obtained from the literature,[8-10] and key simulation parameters are summarized in Table I. Injection efficiency is modeled implicitly in the DD simulations, which determine the fraction of applied current flowing into the quantum well by simulating recombination currents in all layers.

DD results for a broad range of QW and WG lifetimes showed an excellent fit to (5); the coefficients $I_0(V)$ and $I_{WG}(V)$ were very weakly dependent on QW lifetime. For the devices studied here, the ratio of QW to SCH currents I_{QW}/I_{SCH} was 2 to 2.25 over the Van Opdorp linear range. The $I_0(V)$ term in (6) contributed 20 to 30% to the SCH current $(I_0(V) + \frac{1}{\tau_{WG}} I_{WG}(V))$ over the Van Opdorp linear range, which corresponds to less than 10% of the total device current.

Because the device is operated well below transparency in this measurement regime, carrier densities in the waveguide are extremely low and waveguide emission is negligible. The simulations show that waveguide spontaneous emission does not exceed 0.04% of the QW spontaneous emission for a broad range of WG and QW nonradiative lifetimes, indicating that the emission L provides a good measure of QW carrier density in (1) and (6).

Table I: Parameters Used in Drift-Diffusion Simulations

(QW= quantum well, WG= waveguide, CB=conduction band, VB=valence band)

Parameter	Units	Value	Comments
QW bandgap	eV	1.567	Between CB1, VB1 levels
QW CB Density of States	cm^{-3}	7.67 $x10^{17}$	
QW VB Density of States	cm^{-3}	6.41 $x10^{18}$	
QW radiative B coefficient	cm^3/s	2.8 $x10^{-10}$	
QW Auger coefficient	cm^6/s	1.8 $x10^{-30}$	
WG bandgap	eV	1.902	
WG CB Density of States	cm^{-3}	6.91 $x10^{17}$	
WG VB Density of States	cm^{-3}	1.35 $x10^{19}$	
WG radiative B coefficient	cm^3/s	1.0 $x10^{-10}$	
Cladding bandgap	eV	2.20	
Cladding CB Density of States	cm^{-3}	7.52 $x10^{18}$	
Cladding VB Density of States	cm^{-3}	1.57 $x10^{19}$	
WG and QW net doping	cm^{-3}	1.0 $x10^{15}$	n-type, from C-V profile

5.2 Analysis results

Nonradiative lifetimes were determined by minimizing the sum of the residual errors between the measured currents I_K and the model fit values (right hand side of (6)) using Nelder-Mead simplex optimization fit parameter scaling so that all optimized parameters have similar scaled magnitudes. The optimization converges for a wide range of input seeds, provided the initial guess for collection efficiency C is within a factor of ~20 of the true value. We determined an initial guess for C by a linear fit of the data to (2). The fitting standard errors for the parameters were determined from standard deviations of the residual errors and the Hessian matrix of the objective function.

The fitting procedure results in a current fit that closely matches the I-V data in the VanOpdorp linear range, as shown in Figure 2. The root-mean-squared errors on the current residuals from Eq. (6) were 0.15% or less over the Van Opdorp linear region for all devices tested, and the fitting standard errors on the deduced QW and waveguide lifetimes were less than 0.2 ns. The deduced lifetimes depend on the selection of the linear Van Opdorp range used for fitting. This range can be optimized by minimizing the

fit standard error. The effective precision of these measurements is dominated by fit range selection, which we conservatively estimate as ±5 and ±0.8 ns for the QW and waveguide lifetimes, respectively.

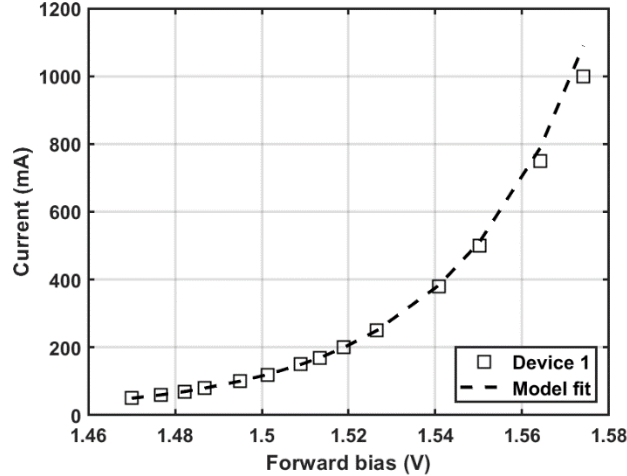

Figure 2: Comparison of the experimental I-V characteristic for Device 1 to a fit of Eq. (6). Deviations at high bias, outside the Van Opdorp linear range, are due to amplification of the spontaneous emission.

Table II shows the deduced lifetime values for the devices investigated. Variations among devices are attributable to manufacturing variability. Our deduced QW lifetimes are consistent with reported QW nonradiative lifetimes, which are mostly available for the AlGaAs material system and span a large range (10~200 ns).[11-15] Our deduced lifetimes for the InGaP waveguide material are somewhat lower than literature values of ~12 ns for bulk, undoped InGaP.[16, 17] Analyzing the same data with the original approach of (3)[1] results in deduced QW lifetimes approximately half as large as those in Table II, between 32 and 49 ns for these devices. While some of this difference results from the finite injection efficiency, which averaged 70 to 80% for these devices in the Van Opdorp linear range, the differences primarily result from the *change* in injection efficiency with bias over the linear range.

Table II: Nonradiative Recombination Lifetimes in the QW and WG for Five Devices

Device Number	Waveguide Lifetime (ns)	Quantum Well Lifetime (ns)
1	9.5	84.6
2	8.0	77.3
3	11.9	70.9
4	9.6	81.3

5.3 Uncertainty analysis

The small fitting standard errors achievable with this method show that it is well suited for measuring nonradiative lifetime changes with high precision; notably, for investigating lifetime changes in a single device as a function of aging or other handling. The absolute accuracy of the method is also of interest; it depends on the fidelity of the assumed material parameters and the DD model. The deduced QW nonradiative lifetime is proportional to $B^{-1/2}$, so uncertainties in the radiative recombination coefficient B affect the accuracy of this method. The radiative recombination coefficient B can be determined to at least 10~20% accuracy, resulting in a QW lifetime uncertainty of 5~10%. The effect of uncertainties in Auger coefficient depends strongly on the material system being investigated. For the structure investigated here, Auger recombination in the Van Opdorp linear range is very small, and this parameter contributes <1% to the deduced nonradiative lifetime uncertainties.

The deduced lifetimes also depend on parameters assumed for the DD model, and uncertainties in these parameters impact the absolute uncertainties of the lifetimes. Model QW composition changes corresponding to 5.6 meV bandgap shifts result in deduced QW and waveguide nonradiative lifetime changes of ~3% and 0.6%, respectively, for the structure investigated here. A 30% increase in the model waveguide net donor density changes the deduced waveguide and QW nonradiative lifetimes by approximately -4% and -8%, respectively. Combining these model uncertainties with the parameter uncertainties and precision described above yields an overall absolute uncertainty below 12% both QW and waveguide lifetimes reported in Table II. These sensitivity studies show that some care must be taken in defining the DD model used to support this characterization method.

5.4 Interpretation

Nonradiative recombination generally exhibits a complex behavior that depends on carrier densities n and p, recombination center energy levels, and the separate capture lifetimes for electrons τ_n and holes τ_p.[2] For the equal carrier lifetime assumption $\tau_n = \tau_p$ used here, it can be shown that the deduced QW lifetime is τ_{QW} $(n+p)/2(np)^{1/2}$ for carrier densities much greater than the intrinsic density and $\tau_{QW} = \tau_n + \tau_p$. While changes in the carrier density ratio n/p will change the effective lifetime, this effect results in relatively small bias dependence. Over the Van Opdorp linear range, it accounts for a τ_{QW} variation no more than 4%, which can be corrected using the QW carrier densities determined from the DD simulator. Larger

effects could result if the electron and hole lifetimes differ significantly; however, a more sophisticated analysis to extract separate τ_n and τ_p values is not warranted because data in the Van Opdorp linear range is fit extremely well with the $\tau_n = \tau_p$ assumption.

The deduced lifetimes represent a weighted average of nonradiative recombination rates at interfaces and in the bulk. The proposed method cannot distinguish interface from bulk recombination without additional measurements in which lifetimes are measured as a function of bulk material dimensions (epilayer thickness, laser stripe width, or laser cavity length). The measured cavity length dependence of devices similar to those studied here shows that facet recombination contributes less than 4% to the overall current in the Van Opdorp linear region.[4]

The proposed measurement approach can also be applied to laser diode bars containing multiple independent diode emitters. In this geometry, all emitters will be biased at the same voltage due to their shared ohmic contacts and the low measurement current. In this case, the deduced QW and waveguide lifetimes represent the average recombination ***rates*** over all emitters. For this geometry, the parameters V* and C in Eqs. (3) and (6) represent the total active volume over all emitters and the average collection efficiency over all emitters, respectively. Derivation of these results is presented in the appendix.

6. Conclusion

In conclusion, a new method has been developed for determination of nonradiative recombination lifetimes in quantum well laser diodes and multi-emitter laser diode bars. This approach characterizes nonradiative lifetimes in both the waveguide and the quantum well, requires no special measurement equipment if the device structure is known, and can be applied to packaged lasers with limited access to the active region. The method assumes that DD simulations capture all relevant physical processes and that lifetimes can be represented as homogenous quantities; it does not resolve spatial dependence of lifetimes within the cavity, nor does it resolve contributions from different recombination center species.

Example measurements demonstrate a high precision of 0.2 ns for measured lifetimes, which renders this approach well suited for studying lifetime changes for a given device subjected to aging or environmental shocks. For laser diodes with integrated monitoring photodetectors, this method could employ signals from the integrated detector to further simplify the metrology, provided that the integrated detector

provides sufficient sensitivity below threshold. The absolute accuracy of the method is determined by uncertainties in model parameters (QW composition, radiative recombination coefficient, waveguide doping, etc.) is approximately 10% for well-characterized device structures. Uncertainties in the absolute values of deduced lifetimes will have only minimal effects on the deduced lifetime *changes* if this method is used to study device changes during aging or other stressors.

Acknowledgement

This work was performed in part under the auspices of U.S. DOE by Lawrence Livermore National Laboratory (LLNL) under Contract No. DE-AC52-07NA27344 and supported in part under Laboratory Directed Research and Development (21-SI-002) at LLNL.

Appendix

Consider a pair of emitters 1,2 that share a common pair of electrodes. Each emitter is assumed to have an active region volume ½ V*, different collection efficiency $C_{1,2}$, and different QW nonradiative lifetime $\tau_{1,2}$. For the low currents used in the linear Van Opdorp range, series resistance effects are small and both emitters will have the same voltage applied to the waveguide. Therefore the QW carrier densities of both emitters N should be the same. Under this assumption, we can apply (6) for each emitter and sum the emitter currents $I_{1,2}$:

$$I = (I_1 + I_2) = I_0(V) + I_{wg}(V)\frac{1}{2}(\tau_{WG1}^{-1} + \tau_{WG2}^{-1}) + eV^*\left(\frac{1}{2}(\tau_{WG1}^{-1} + \tau_{WG2}^{-1})N + BN^2\right) \quad (7)$$

with photon output $L = L_1 + L_2 = \frac{1}{2}(C_1 + C_2)V^*BN^2 = CV^*BN^2$. This demonstrates that the nonradiative lifetimes deduced for a multi-emitter laser diode bar represent averages of the recombination rates, provided that the analysis uses the total active QW volume V* (summed over all emitters) and the average collection efficiency over all emitters.

Data availability statement

The data that support the findings of this study are available from the corresponding author upon reasonable request.

Author declarations

Authors Thaler, Song, Crowley, and Thiagarajan are employees of Leonardo Electronics, Inc., a manufacturer of laser

diode devices, and hence hold an interest in the financial performance of the company.

REFERENCES

1. C. van Opdorp and G. W. ’t Hooft, Journal of Applied Physics **52** (6), 3827-3839 (1981).
2. C. T. Sah, R. N. Noyce and W. Shockley, Proceedings of the Institute of Radio Engineers **45** (9), 1228-1243 (1957).
3. J. Nelson, I. Ballard, K. Barnham, J. P. Connolly, J. S. Roberts and M. Pate, Journal of Applied Physics **86** (10), 5898-5905 (1999).
4. W. E. Fenwick, R. J. Deri, S. H. Baxamusa, D. L. Pope, M. C. Boisselle, D. M. Dutra, N. P. Allen, M. Crowley, P. Thiagarajan and T. Hosoda, Semiconductor Science and Technology **37** (9) (2022).
5. M. C. Delong, D. J. Mowbray, R. A. Hogg, M. S. Skolnick, M. Hopkinson, J. P. R. David, P. C. Taylor, S. R. Kurtz and J. M. Olson, Journal of Applied Physics **73** (10), 5163-5172 (1993).
6. K. I. Kolokolov, A. M. Savin, S. D. Beneslavski, N. Y. Minina and O. P. Hansen, Physical Review B **59** (11), 7537-7545 (1999).
7. L. A. Coldren, S. W. Corzine and M. L. Masonovic, in *Diode Lasers and Photonic Integrated Circuits* (2012), pp. 157-246.
8. I. Vurgaftman and J. R. Meyer, Journal of Applied Physics **94** (6), 3675-3696 (2003).
9. M. Sotoodeh, A. H. Khalid and A. A. Rezazadeh, Journal of Applied Physics **87** (6), 2890-2900 (2000).
10. A. T. Meney, A. D. Prins, A. F. Phillips, J. L. Sly, E. P. Oreilly, D. J. Dunstan, A. R. Adams and A. Valster, Ieee Journal of Selected Topics in Quantum Electronics **1** (2), 697-706 (1995).
11. S. C. Lee, Y. F. Zhao, R. D. Schrimpf, M. A. Neifeld and K. F. Galloway, Ieee Transactions on Nuclear Science **46** (6), 1797-1803 (1999).
12. B. Sermage, F. Alexandre, J. Beerens and P. Tronc, Superlattices and Microstructures **6** (4), 373-376 (1989).
13. A. Hariz, P. D. Dapkus, H. C. Lee, E. P. Menu and S. P. Denbaars, Applied Physics Letters **54** (7), 635-637 (1989).
14. K. W. J. Barnham, I. Ballard, J. P. Connolly, N. J. Ekins-Daukes, B. G. Kluftinger, J. Nelson and C. Rohr, Physica E-Low-Dimensional Systems & Nanostructures **14** (1-2), 27-36 (2002).
15. K. H. Lee, K. W. J. Barnham, J. S. Roberts, D. Alonso-Alvarez, N. P. Hylton, M. Fuhrer and N. J. Ekins-Daukes, Ieee Journal of Photovoltaics **7** (3), 817-821 (2017).
16. F. J. Schultes, T. Christian, R. Jones-Albertus, E. Pickett, K. Alberi, B. Fluegel, T. Liu, P. Misra, A. Sukiasyan, H. Yuen and N. M. Haegel, Applied Physics Letters **103** (24) (2013).
17. A. Toda, K. Nakano, T. Yamamoto and M. Ikeda, Applied Physics Letters **66** (25), 3483-3485 (1995).